JOURNAL OF THE ROYAL SOCIETY Interface

J. R. Soc. Interface (2011) **8**, 1785–1795
doi:10.1098/rsif.2011.0144
Published online 20 May 2011

Effects of flow and colony morphology on the thermal boundary layer of corals

Isabel M. Jimenez[1], Michael Kühl[1,2], Anthony W. D. Larkum[1,3] and Peter J. Ralph[1,*]

[1]*Plant Functional Biology and Climate Change Cluster (C3), Department of Environmental Science, University of Technology, Broadway, Sydney, New South Wales 2007, Australia*
[2]*Marine Biological Section, Department of Biology, University of Copenhagen, Strandpromenaden 5, 3000 Helsingør, Denmark*
[3]*School of Biological Sciences, University of Sydney, Heydon-Laurence Building A08, Sydney, New South Wales 2006, Australia*

The thermal microenvironment of corals and the thermal effects of changing flow and radiation are critical to understanding heat-induced coral bleaching, a stress response resulting from the destruction of the symbiosis between corals and their photosynthetic microalgae. Temperature microsensor measurements at the surface of illuminated stony corals with uneven surface topography (*Leptastrea purpurea* and *Platygyra sinensis*) revealed millimetre-scale variations in surface temperature and thermal boundary layer (TBL) that may help understand the patchy nature of coral bleaching within single colonies. The effect of water flow on the thermal microenvironment was investigated in hemispherical and branching corals (*Porites lobata* and *Stylophora pistillata*, respectively) in a flow chamber experiment. For both coral types, the thickness of the TBL decreased exponentially from 2.5 mm at quasi-stagnant flow (0.3 cm s^{-1}), to 1 mm at 5 cm s^{-1}, with an exponent approximately 0.5 consistent with predictions from the heat transfer theory for simple geometrical objects and typical of laminar boundary layer processes. Measurements of mass transfer across the diffusive boundary layer using O_2 microelectrodes revealed a greater exponent for mass transfer when compared with heat transfer, indicating that heat and mass transfer at the surface of corals are not exactly analogous processes.

Keywords: coral; temperature; boundary layer; water flow; microsensor

1. INTRODUCTION

In shallow reef environments, the ambient water temperature can underestimate the heat exposure of corals [1,2]. During periods of low wind, clear skies and low turbidity, a combination of limited water circulation and strong light penetration into the water column (e.g. [3]) can elevate the temperature of individual corals above that of the surrounding water by up to 1°C [1,2]. Such an apparently minor heating effect can be of great significance to corals, which generally thrive optimally only 1–2°C below their maximal temperature tolerance [4,5]. Microenvironmental thermal stress, induced under high irradiance and low water flow, has hitherto been largely overlooked, but may be of particular importance for understanding and monitoring heat-induced stress on coral reefs. Clear and calm weather conditions in shallow reefs, when the ambient water temperature can rise by several degrees, are often associated with the onset of coral bleaching breaking down the coral symbiosis with their zooxanthellae and potentially resulting in widespread coral mortality (e.g. [3,6]). Large-scale bleaching events have occurred at increasing frequency in the past 30 years [7,8] and seem closely linked to global warming [9]. The role of the thermal microenvironment of corals in such heat stress responses is unknown.

Solar-induced heating of corals can be reduced by increased flow velocity, and is also influenced by coral colour as well as their shape and size [1,2]. A better understanding of the temperature differences that may arise between individual corals during and prior to a bleaching event would refine the spatial and temporal accuracy of temperature monitoring programmes based on measurements of sea surface temperature (e.g. NOAA Coral Reef Watch Programme, [10]). To assist monitoring programmes, it is expected that a coral thermal model, based on principles of heat transfer theory, could estimate the temperature variability of corals in the field [2]. However, such a model requires that the effects of environmental parameters such as irradiance, and in particular water flow, are adequately described in mathematical terms.

*Author for correspondence (peter.ralph@uts.edu.au).

Received 16 March 2011
Accepted 27 April 2011

The rate of convective heat loss at the surface of corals is limited by the presence of a thermal boundary layer (TBL), which extends a few millimetres from the coral surface [2]. The TBL acts as an insulating barrier where conductive heat transfer may dominate over advection [11]. The surface warming of corals is thus modulated by the thickness of the TBL, which typically decreases with the inverse power of the flow velocity [2,12]. However, the exact formulation of this power-law relationship between TBL thickness and flow is specific to the shape of the submerged object, the topography of the surface of exchange and the physical characteristics of the water flow (velocity and turbulence level). While such relationships are known for simple geometrical shapes such as spheres and cylinders [12], they need to be determined empirically for complex structures such as corals.

The TBL emerges through the interaction of the coral's surface with the viscous forces in the fluid [11], and is therefore analogous to the diffusive boundary layer (DBL) that controls the exchange of solutes and dissolved gases (such as O_2) between corals and the surrounding water [13–15]. In a previous study [2], we showed the presence of a TBL and a DBL at the surface of corals, and verified that the TBL was approximately four times thicker than the DBL, as expected from heat and mass transfer theory. The theoretical analogy between heat and mass transfer implies that despite the different spatial scales of the TBL and DBL, the thickness of both boundary layers should respond in a similar way to increasing flow velocity [12]. The power-law relationship between flow velocity and boundary layer thickness is often considered interchangeable between heat and mass transfer processes [2,12,16]. Consequently, the mathematical relationship describing the TBL thickness (δ_{TBL}) as a function of flow could in theory be inferred from the analogous relationship between DBL thickness (δ_{DBL}) and flow, which has been characterized for oxygen transfer at the surface of branching (*Pocillopora damicornis* [6]) and hemispherical corals (*Montastrea annularis* [16]). However, for such relationships to be reliably translated from one process to the other, the validity of the heat-mass transfer analogy should first be verified for corals, with their complex surface topographies and shapes.

In order to better understand and ultimately predict the thermal exposure of individual corals under bleaching conditions, we investigated the effect of water flow on the temperature of shallow-water corals. Microsensor technology was used in two controlled laboratory experiments to (i) examine the effect of coral surface topography on the temperature microenvironment at the scale of individual polyps in *Leptastrea purpurea* and *Platygyra sinensis*; and to (ii) empirically determine the mathematical relationship between water velocity and the thickness of the TBL for two coral species with contrasting morphology: the branching *Stylophora pistillata* and the hemispherical *Porites lobata*; and (iii) compare the responses of the TBL and the DBL to variations in flow velocity.

2. MATERIAL AND METHODS

2.1. Corals

Corals were collected in January 2007 from the shallow lagoon adjacent to Heron Island Research Station, Great Barrier Reef, Australia (151°55′ E, 23°26′ S) and maintained in continuously flowing sea water at 26°C, i.e. the ambient lagoon temperature. For contour mapping of the TBL over individual polyps (experiment 1), corals with rough topographies were chosen (figure 1): a small colony of *L. purpurea* (approx. 35 mm in diameter) characterized by rounded approximately 1 mm deep corallites and a small *P. sinensis* colony (approx. 45 mm in diameter), characterized by approximately 2 mm deep valleys and ridges. Corals of relatively smooth topography, characterized by small and shallow polyps (less than 1 mm), were collected and transported to Sydney for experimental work on the effects of flow on the TBL and DBL (experiment 2): 10 colonies of *P. lobata* (approx. 35 mm in diameter) and nine fragments of *S. pistillata* (approx. 50 mm in length, each with one to three branches; branch thickness 5–6 mm).

2.2. Boundary layer measurements

Temperature and O_2 boundary layers were investigated using the microsensor profiling equipment and experimental set-up described in Jimenez *et al.* [2] and in more detail for each experiment (see below). Briefly, corals were each placed in a Plexiglas flow chamber (see below for chamber dimensions in each experiment) flushed with aerated sea water (25°C, salinity of 33). Actinic light (400–800 nm) was provided by either a fibre optic light source (Schott KL-2500, Germany) or a halogen lamp (PAR38150W, Arlec, Australia).

For TBL measurements, a temperature microsensor with a tip size of 50 µm (TP50 microthermocouple, Unisense A/S, Aarhus, Denmark) was connected to a thermocouple meter (T301, Unisense A/S) and mounted on a motorized micromanipulator (Märtzhäuser, Wetzlar, Germany) with computerized depth control. For O_2 DBL measurements (experiment 2 only), a Clark-type O_2 microelectrode with a tip diameter of 10 µm (OX10, Unisense A/S) was connected to a picoammeter (PA2000, Unisense A/S) and calibrated linearly using sensor readings in air-saturated sea water and O_2-free sea water, respectively. Data acquisition was done via an analogue/digital converter interfaced to a PC running software for positioning and data acquisition (Profix, Unisense A/S). A dissecting microscope (Leica, Wetzlar, Germany) was used to position the microsensor tip at the surface of the coral tissue before commencement of vertical profiling.

Because the temperature and O_2 concentration profiles were nonlinear (figure 2), the hyperbolic tangent method of Nishihara & Ackerman [18,19]) was used to determine the thickness of the TBL, δ_{TBL}, and of the DBL, δ_{DBL}. Dimensionless profiles ($\Theta(z)$) were calculated as

$$\Theta(z) = \frac{X - X_s}{X_w - X_s}, \tag{2.1}$$

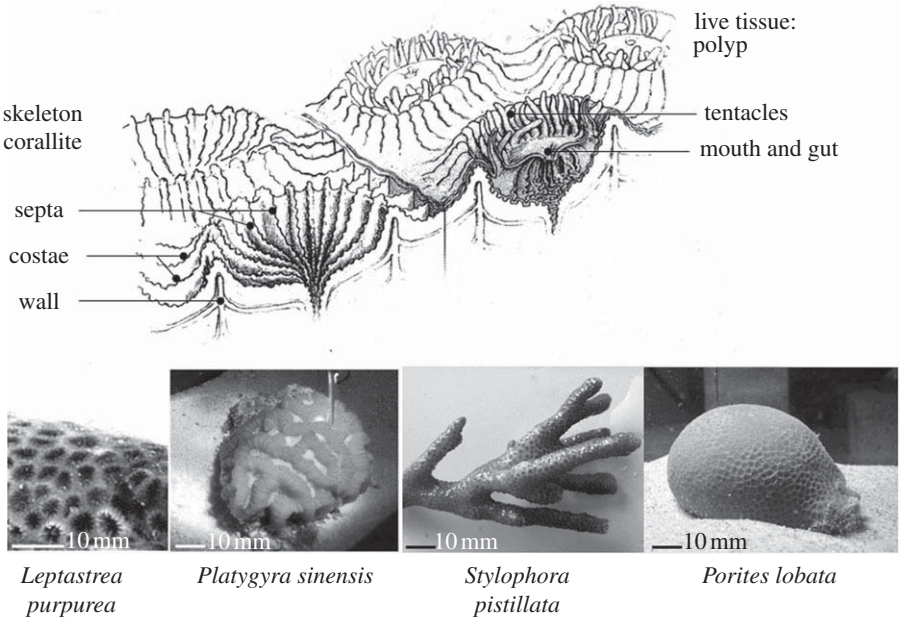

Figure 1. Schematic of the typical surface features of a coral, showing details of the skeleton corallites secreted by the soft tissue of individual polyps (modified with permission from Kelley [17]). Photographs of the morphologically distinct coral species used in the flow chamber experiments: *L. purpurea* and *P. sinensis* were used for mapping of the thermal microenvironment of corals of complex surface topography, while the relatively smooth, branching *S. pistillata* and hemispherical *P. lobata* were used to assess the effect of flow velocity on the TBL thickness.

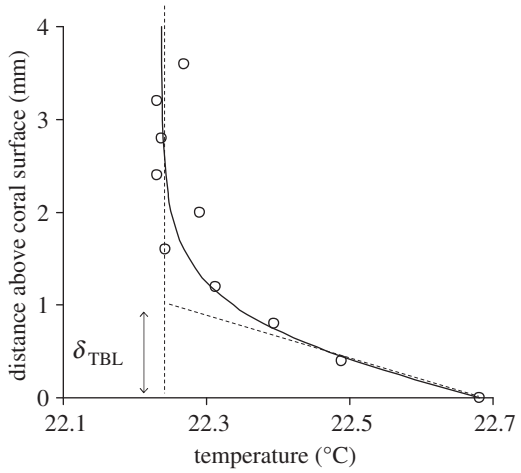

Figure 2. Typical temperature profile (open circles) over a hemispherical *P. lobata* exposed to a flow velocity of 0.6 cm s^{-1} and an irradiance of 1500 W m^{-2}, fitted hyperbolic tangent curve (solid line) and estimate of the effective thickness of the thermal boundary layer, δ_{TBL}, as the intersection between the tangent at z=0 and the constant water temperature in the free-flowing water above the coral.

where X is the temperature (T) or O_2 concentration (C), and the subscripts s and w denote the value at the coral surface and in the bulk water stream, respectively. A hyperbolic tangent function was then fitted to the dimensionless profiles

$$\Theta(z) = B \tanh\left(\frac{A}{B} z\right), \tag{2.2}$$

where A and B are constants. The effective thicknesses of the TBL, δ_{TBL}, and the DBL, δ_{DBL}, were estimated as the intersection between the profile tangent at the coral surface and the constant value in the free-flowing water above the corals (figure 2).

Therefore,

$$\left.\frac{dX}{dz}\right|_{z=0} = \frac{X_w - X_s}{\delta}. \tag{2.3}$$

The derivative of equation (2.2) evaluated at $z = 0$ gives

$$\left.\frac{d\Theta}{dz}\right|_{z=0} = A. \tag{2.4}$$

And thus

$$\left.\frac{dX}{dz}\right|_{z=0} = (X_w - X_s)\left.\frac{d\Theta}{dz}\right|_{z=0} = (X_w - X_s)A. \tag{2.5}$$

Inserting this result into equation (2.3) results in the expression used to estimate the thicknesses of the TBL and the DBL:

$$\delta = \frac{1}{A}. \tag{2.6}$$

2.3. Experiment 1. Polyp-scale thermal microenvironment

The *L. purpurea* and *P. sinensis* specimens were each exposed to a flow velocity of 1 cm s^{-1} in a Plexiglas flow chamber (10 × 5 × 25 cm) flushed with aerated sea water (25°C; salinity 33). Downwelling irradiance was provided by a fibre optic light source (Schott KL-2500) fitted with a collimating lens and a heat filter. Corals were exposed to 430 W m^{-2} (measured in air with a pyranometer, LiCor, Nebraska, USA), corresponding to 1500 μmol photons m^{-2} s^{-1} (measured in air with a

LI-1400 datalogger and LI-190SA quantum sensor, LI-COR). Temperature contour maps were constructed from multiple temperature microprofiles ($n = 7$–9) measured at 0.5–1 mm horizontal intervals and 200 µm vertical intervals along a transect across a single polyp and perpendicular to the direction of flow. The coordinates of the tissue surface were determined for each profile by positioning the microsensor tip at the surface using a micromanipulator (Märtzhäuser, Germany) and observation through a dissecting microscope.

2.4. Experiment 2. Flow effects on the thermal boundary layer and diffusive boundary layer

The effect of flow on the TBL and DBL of *P. lobata* and *S. pistillata* was investigated using a longer flow chamber (Plexiglas, $10 \times 5 \times 36$ cm) that permitted flow velocities up to 5 cm s^{-1}. For the TBL measurements, corals were heated by strong irradiance (1500 W m^{-2}, corresponding to approx. 2500 µmol photons m^{-2} s^{-1}) provided by a halogen lamp (PAR38150W, Arlec, Australia). Extreme levels of irradiance, while not environmentally realistic, were chosen for measurements of the TBL in order to ensure sufficient heating and well-defined temperature profiles even at increased flow velocities. The corals were exposed to seven different flow velocities (0.3, 0.6, 1.4, 2.3, 3.0, 3.8 and 5.0 cm s^{-1}), as determined by visual tracking of neutrally buoyant particles (brine shrimp cysts) in the free stream 2 cm above the corals. The hemispherical *P. lobata* colonies were oriented in the direction of the flow, while the branches of *S. pistillata* were oriented horizontally and perpendicularly to the direction of flow. All corals were placed at the same position within the flow chamber. Three replicate temperature microprofiles (measured at intervals of 50–200 µm vertical distance) were performed after 15 min incubation at each flow velocity; the same point on the coral's upper surface was sampled at all flows. Additional profile measurements (data not shown) over a 1 cm^2 tissue area on the light-exposed region of the coral surface confirmed that the relatively smooth topography of *P. lobata* and *S. pistillata* only caused a small spatial variation in δ_{TBL} of approximately 10 per cent, unlike *L. purpurea* and *P. sinensis*.

Measurements of the O_2 DBL were performed a week later using the same flow chamber and the exact same coral individuals, positioned and oriented as for the previous TBL measurements, and exposed to each of five flow velocities: 0.5, 0.7, 1.3, 3.7, 4.3 cm s^{-1} under a downwelling irradiance of 430 µmol photons m^{-2} s^{-1}, provided by a fibre optic light source (Schott KL-2500).

2.5 Coral reflectance spectra

In order to account for potential differences in radiative absorption [1] between the two groups of corals, the reflectance spectrum (400–750 nm; 0.35 nm spectral resolution) of each coral was measured with a fibre-optic spectrometer (USB2000, Ocean Optics, USA) equipped with a 1.5 mm diameter bifurcated fibre-optic reflectance probe (R400-7-UV/VIS, Ocean Optics). Each coral was submersed in filtered sea water in a small glass beaker filled with 0.45 µm filtered sea water, and the tip of the probe was positioned approximately 5 mm and at a 90° angle relative to the coral surface. Actinic light (400–800 nm) was provided by a deuterium-halogen light source (DH-2000-BAL, Ocean Optics) connected to the input branch of the bifurcated reflectance probe, while the reflected light was collected through the input branch. Based on a numerical aperture of 0.22, the input branch thus collected light over a solid angle of approximately 0.1 sr, which at the measuring distance projected to a circular area (field of view) of approximately 2 mm^2.

Spectral reflectance (R) was measured as the ratio of reflected light from the coral surface to that reflected from a 99 per cent diffuse reflectance standard (Spectralon, Labsphere, USA). Spectral reflectance was then further normalized to the reflectance at 750 nm. Potential differences in reflectance spectra caused by variations in the distance of the probe to the coral surface, or differential skeletal scattering properties between the branching and the massive species would be apparent at wavelengths greater than 700 nm where absorption by the pigmented coral tissue is minimal [20,21]. Normalization to the reflectance at 750 nm corrected for such variations and enabled comparison of the optical absorption properties of the tissue of *P. lobata* and *S. pistillata*. Subsequently, normalized reflectance spectra (R) were averaged over 400–700 nm and the average tissue absorptivity, i.e. the fraction of absorbed irradiance was estimated as $\alpha = 1 - R$.

3. RESULTS

3.1. Experiment 1

3.1.1. Thermal boundary layer mapping. The thickness of the TBL over individual polyps of *P. sinensis* and *L. purpurea* was strongly affected by topographical features of the corallites such as protruding septae (figure 3). For *P. sinensis*, the TBL over polyp tissue was thicker than over the coenosarc (i.e. the connective tissue separating adjacent polyps; figure 3*a*) and for both species, regions of polyp tissue were up to 0.3°C warmer than the coenosarc (figure 3*a*,*b*).

3.2. Experiment 2

3.2.1. Coral surface temperature. The surface temperature of *S. pistillata* branches and of hemispherical specimens of *P. lobata* (figure 4) increased above that of the surrounding water by up to +0.20°C and +0.55°C, respectively, when exposed to high irradiance (1500 W m^{-2}, corresponding to approx. 2500 µmol photons m^{-2} s^{-1}) and quasi-stagnant flow (0.3 cm s^{-1}). Warming of the coral surface decreased with increasing velocity down to approximately 0.05°C and 0.10°C (for each species, respectively) at a flow of 5 cm s^{-1} (figure 4). Curve fitting of the experimental data showed that the relation between coral surface warming, ΔT, and flow velocity, u, followed a power-law relationship of the form: $\Delta T \sim u^{-m}$, where the exponent m was approximately 0.5 (figure 4). Such a relation is in agreement with heat transfer theory [12] and the exponent is consistent with heat transfer across a laminar boundary

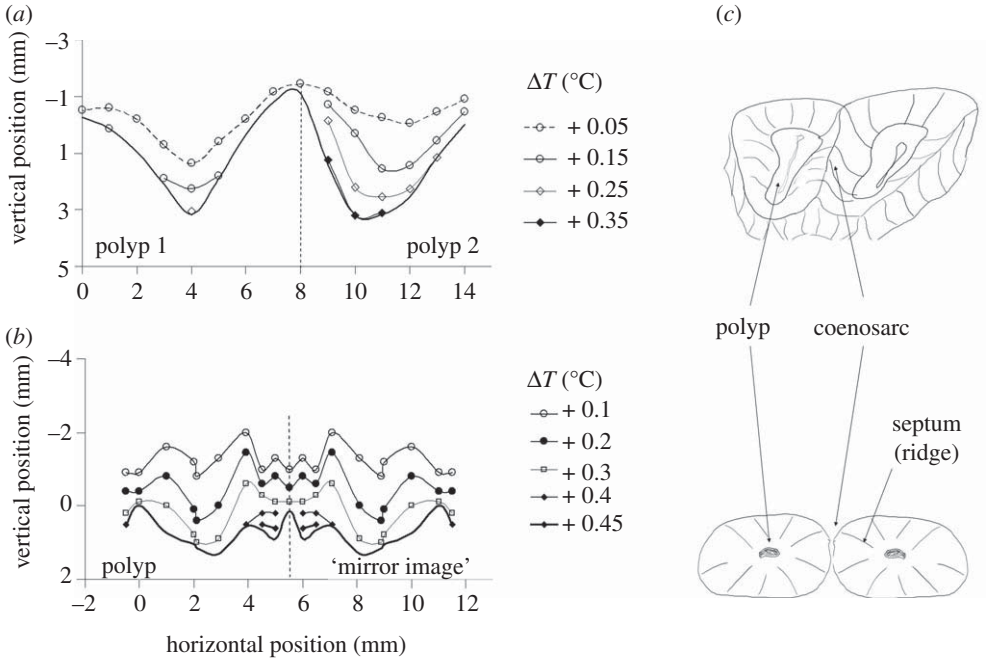

Figure 3. Contour maps of the thermal boundary layer over (*a*) two neighbouring polyps of *P. sinensis* and (*b*) an individual polyp of *L. purpurea*, under flow and light conditions of 1 cm s^{-1} and 430 W m^{-2} (approx. 1500 µmol photons m^{-2} s^{-1}), respectively. For better illustration, the map for *L. purpurea* was duplicated by right symmetry. (*c*) Schematic of polyps of the *P. sinensis*. and *L. purpurea* specimens. ΔT (°C): dashed line with open circles, +0.05; solid line with open circles, +0.15; solid line with open diamonds, +0.25; solid line with filled diamonds, +0.35.

layer [22]. At all experimental flow rates, the thickness of the TBL measured on the colony's apex was similar for both coral species, but the hemispherical *P. lobata* experienced a greater surface warming than the thin branches of *S. pistillata* (figure 5).

3.2.2. O_2 concentration at the coral tissue surface. The tissue surface O_2 concentration of *S. pistillata* and *P. lobata* (exposed to 430 µmol photons m^{-2} s^{-1}) decreased with increasing flow velocity, i.e. from 199 and 209 per cent air saturation, respectively, at quasi-stagnant flow (0.3 cm s^{-1}), down to 122 and 139 per cent air saturation, respectively, at 4 cm s^{-1} (figure 6). The relationship between flow velocity, u, and O_2 surface concentration, C_s, could also be described by a power law of the form $C_s \sim u^{-m}$, with $m = \sim 0.2$.

3.2.3. Thermal and diffusive boundary layers. The effective TBL thickness (δ_{TBL}) of both species ranged from 0.7 to 2.0 mm (figure 7*a,b*) and followed a power-law relationship with flow similar to that of the coral surface warming (figure 4). The δ_{TBL} of *P. lobata* and *S. pistillata* were similar at all sampled flows, except at quasi-stagnant flow (0.3 cm s^{-1}) where *P. lobata* had a thicker TBL than *S. pistillata* (figure 6*a,b*). The effective DBL thickness (δ_{DBL}) was similar for both species (figure 7*a,b*) and varied from 0.2 mm at 4.3 cm s^{-1} to 0.7 mm at 0.5 cm s^{-1}. The DBL was thus thinner than the TBL by a factor of 2.9–3.5. A power-law relationship with flow was also found for the DBL thickness (figure 7*a,b*), as expected from mass transfer theory and numerous experimental reports of mass transfer processes in corals (e.g. [6,16,23]).

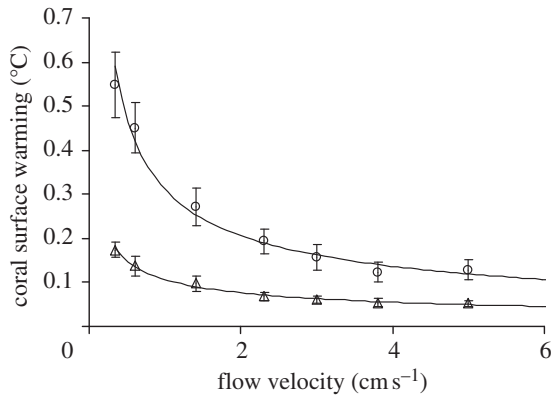

Figure 4. Effect of flow on the tissue surface warming of *S. pistillata* (open triangles) branches ($n = 9$) and hemispherical colonies of *P. lobata* (open circles) ($n = 10$), measured in a flow chamber under high irradiance (1500 W m^{-2}; approx. 2500 µmol photons m^{-2} s^{-1}). Symbols with error bars represent averages ± s.e. The least-square power-law regressions are: $\Delta T = 0.11\ u^{-0.47}$, $r^2 = 0.99$ and $\Delta T = 0.31\ u^{-0.59}$, $r^2 = 0.98$ for *S. pistillata* and *P. lobata*, respectively.

The heat transfer exponents for *S. pistillata* and *P. lobata* were 0.36 ± 0.05 ($n = 9$ ± s.e.) and 0.38 ± 0.03 ($n = 10$ ± s.e.), respectively. They were statistically similar to the expected value of 0.5 for heat transfer across a laminar TBL [12], and were unaffected by coral shape ($p > 0.05$; Student's *t*-test). The mass transfer exponents for both coral species (0.74 ± 0.14 and 0.84 ± 0.12, for *S. pistillata* and *P. lobata*, respectively) were also unaffected by coral shape ($p > 0.05$; Student's *t*-test), but were significantly higher than 0.5 ($p < 0.005$; Student's *t*-test) and typical of transport across a turbulent boundary layer [22].

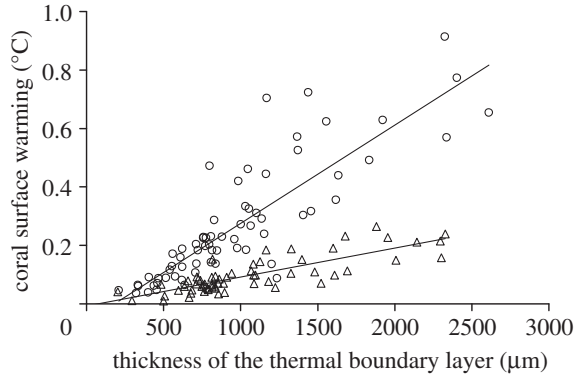

Figure 5. Coral surface warming of *S. pistillata* (open triangles) branches ($n = 9$) and hemispherical colonies of *P. lobata* (open circles) ($n = 10$) plotted against the thickness of the thermal boundary layer, measured under 1500 W m^{-2} (approx. 2500 µmol photons m^{-2} s^{-1}) irradiance and flows ranging between 0.3 and 5 cm s^{-1}. Symbols with error bars represent averages ± s.e. The least-square regression lines are: $\Delta T = 9.9 \times 10^{-5}\ \delta_{TBL} - 7.8 \times 10^{-3}$, $r^2 = 0.67$ and $\Delta T = 3.4 \times 10^{-4}\ \delta_{TBL} - 6.0 \times 10^{-2}$, $r^2 = 0.72$ for *S. pistillata* and *P. lobata*, respectively.

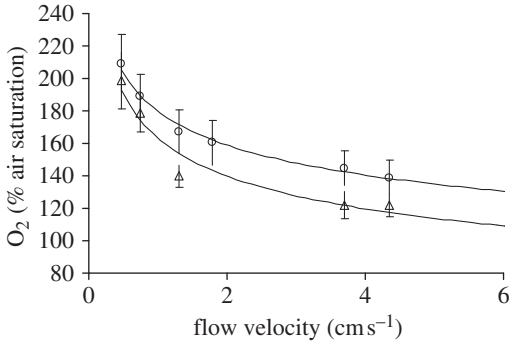

Figure 6. Effect of flow on the surface O_2 concentration of *S. pistillata* (open triangles) branches ($n = 7$) and hemispherical colonies of *P. lobata* (open circles) ($n = 8$), measured in a flow chamber and exposed to 430 µmol photons m^{-2} s^{-1}. Symbols with error bars represent averages ± s.e. The least-square power-law regressions are: $C_s = 163\ u^{-0.22}$, $r^2 = 0.94$ and $C_s = 180\ u^{-0.18}$, $r^2 = 0.99$ for *S. pistillata* and *P. lobata*, respectively.

3.2.4. Coral absorptivity. No significant difference in the coral absorptivity (α) was detected between *S. pistillata* and *P. lobata*: 0.54 ± 0.03 ($n = 9$ ± s.e.) and 0.59 ± 0.02 ($n = 10$ ± s.e.), respectively ($p > 0.05$; Student's *t*-test), thus indicating that the tissue of both coral species had similar light-absorbing efficiencies.

4. DISCUSSION

Earlier studies have shown that flow velocity enhances mass transfer at the tissue surface of corals for a variety of parameters, such as O_2 flux [23–25], inorganic carbon delivery [6], nutrient uptake [26–28] and prey capture [29–31]. The modulation of mass transfer across DBLs by flow is known to affect coral physiology [13,25,32,33], and high water flow has been shown to reduce photoinhibition in corals [34]. The latter observation has been linked to an apparently improved resistance and resilience to bleaching of corals in high flow areas [35–37]. Despite the sensitivity of corals to small increases in temperature [9,38,39], the effect of flow velocity and coral shape on the TBL of corals has hitherto only been briefly addressed [1,2].

4.1. Intra-colonial heterogeneity in thermal boundary layers

Temperature microprofiles showed that the interaction of flow with the coral's topography can result in millimetre-scale heterogeneity in the coral TBL thickness and tissue temperature (figure 3). This is consistent with analogous reports of complex O_2 DBLs over individual polyps [13,33,40]. It remains to be seen how variations in coral topography may influence, for example, the response of TBLs to increases in flow velocity. While our results indicate that deep hollow calices may have the potential to retain a substantial TBL (figure 3*b*), even at higher flows (as seems to be the case for DBLs, cf. [40]), small roughness elements also have the potential to enhance heat fluxes by affecting flow patterns [16] and generating turbulence in the TBL.

These results, together with evidence of intra-colonial variability in O_2 saturation [13,40,41] and light microclimate [13,41], clearly demonstrate that the physico-chemical environment of coral tissue is spatially complex at the scale of individual polyps. This may help understand the patchy nature of coral bleaching at the scale of single colonies. Finally, results from this study indicate that laboratory-based bleaching experiments using heaters to increase the temperature of the surrounding water may not adequately replicate the microscale thermal environment of shallow-water corals *in situ*.

4.2. Flow effects on coral surface temperature

Our results confirm that the surface temperature of corals is most likely to exceed that of the surrounding water under conditions of low flow velocities (less than 5 cm s^{-1}) and high irradiance (figure 4). Flow regimes in coral reefs are extremely variable [14,42], ranging from strong (20–50 cm s^{-1}) wave-generated bidirectional flows on a seaward reef crest to low unidirectional flows (less than 5 cm s^{-1}) in deep fore-reef and shallow back-reef habitats [43]. For the particular case of shallow lagoons and reef flats with minimal wave action, tidally driven flows range from 1 to 15 cm s^{-1} (e.g. [16,44]) and are typically lowest (5 cm s^{-1}or less) during low tide [44,45]. Therefore, the temperature of shallow-water corals is most likely to increase above that of the surrounding water during summer midday low tides, when conditions of low flow and high irradiance coincide.

The dependency of coral surface temperature on flow could be described by an inverse power-law relationship, in accordance with heat transfer theory [12]. A consequence of the power law (e.g. [11]) is that small variations in flow velocity affect the temperature of corals much more efficiently at the lowest flow (less than 2 cm s^{-1}) compared with higher flows (greater than 2 cm s^{-1}; figure 4). Extreme conditions of

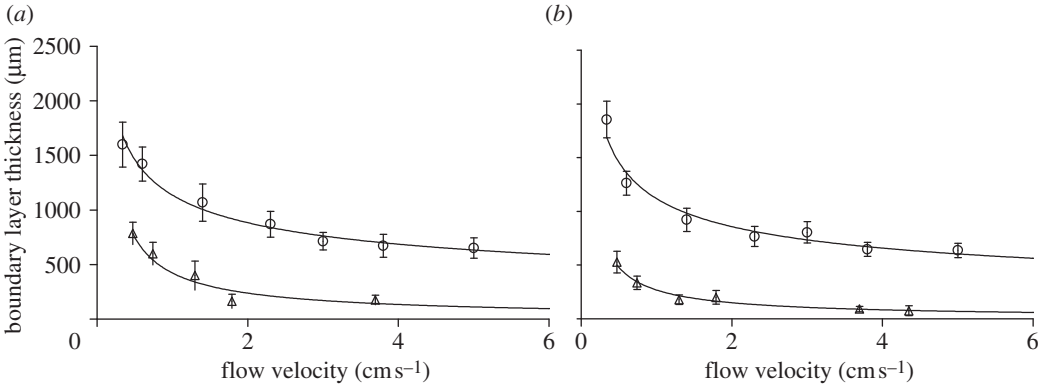

Figure 7. Effect of flow on δ_{TBL} and δ_{DBL} over *S. pistillata* branches (n=9) and hemispherical colonies of *P. lobata* (n=10). Symbols with error bars represent averages ± s.e. The least-square power-law regressions are: (*a*) *S. pistillata*: TBL=1137 $u^{-0.36}$, r^2=0.98 and DBL=469 $u^{-0.74}$, r^2=0.99; (*b*) *P. lobata*: TBL=1118 $u^{-0.38}$, r^2=0.96 and DBL=268 $u^{-0.84}$, r^2=0.97. Open circles, thermal boundary layer; open triangles, oxygen diffusive boundary layer.

quasi-stagnant flow typically occur during particularly calm weather conditions such as doldrums and are often associated with the onset of bleaching [3,9,46]. Our results indicate that under such bleaching conditions, small local variations in flow velocity could greatly affect the temperature of individual corals. Additionally, the three-dimensional structure of the reef creates a wide range of microhabitat flow regimes [42]. In particular, individual corals sheltered within larger aggregations and individual branches within colonies may experience a greatly reduced flow compared with the free stream [6,47]. The temperature of shallow-water corals may thus be spatially variable, and may contribute in part to the flow-related variability in bleaching responses of corals over spatial scales of 1–100 m (e.g. [9,37]).

4.3. Interspecific variability in coral heat budgets

Our flow experiments provided further evidence that interspecific differences in coral morphology can affect a coral's thermal environment as first suggested by Jimenez *et al.* [2]. The temperature of the massive *P. lobata* was consistently higher than that of *S. pistillata* branches, at all flows (figure 4). A similar result was reported in Jimenez *et al.* [2] where the temperature of hemispherical corals was higher than that of the branching specimens. This could be attributed to differences in light-absorption capacity, which may be dynamic, species-specific and seasonally dependent [48–51]. However, in this particular study, no difference in absorptivity was found between the two experimental coral groups, possibly as a result of the acclimation period under artificial light and aquarium growth conditions prior to commencement of measurements.

Temperature differences may also be attributed to variations in the thickness of the TBL [2]. Again, in the present study, the TBL thickness did not differ significantly between massive and branching corals, thus indicating similar efficiencies of convective heat transfer despite their differences in size and shape. Considering that the surface temperature of a coral is controlled by energy exchange with its surroundings, in the form of radiative transfer, heat convection to the water and heat conduction to the skeleton [2], and that the efficiencies of the first two processes were similar among the two coral groups, our results may be attributed to interspecific differences in the efficiency of heat conduction into the skeleton. This is supported by predictions from a simple theoretical coral thermal model described in Jimenez *et al.* [2], together with observations of the slopes of the ΔT versus δ_{TBL} relationships in figure 5. The surface warming of a coral was described in Jimenez *et al.* [2] as a function of the incident irradiance (E), the absorptivity of coral tissue (α), the convection coefficient (h) and a constant K_0, which is a function of heat conduction into the skeleton [2]:

$$\Delta T = \frac{E\alpha}{hK_0}. \tag{4.1}$$

Considering that the convection coefficient can be expressed as an inverse relationship of the thickness of the TBL (i.e. $h=k/\delta_{TBL}$; [11]), equation (2.5) can be written as

$$\Delta T = \frac{\delta_{TBL} E\alpha}{kK_0}. \tag{4.2}$$

Therefore, for a given irradiance (E), the slope of the relationship between coral surface warming (ΔT) and TBL thickness (δ_{TBL}) in figure 5 should be proportional to the coral's absorptivity (α), and inversely proportional to the thermal conductivity of water (k) and the constant K_0. Considering that E and k were held constant, and that no difference was found for δ_{TBL} and α between the coral groups, equation (4.2) suggests that the different slopes in the ΔT versus δ_{TBL} plots (figure 5) are due to differences in the parameter K_0, which is a function of heat conduction into the skeleton. Therefore, although potential effects of coral size and/or colour cannot be completely ruled out [2], our results from this particular experiment indicate interspecific differences in conduction into the skeleton. Thermal properties of the coral skeleton may thus significantly affect the surface heat budget of a coral.

The thermal conductivity of the porous aragonite skeleton should lie between 2.4 and 0.62 $W\,m^{-1}\,K^{-1}$ (for water and aragonite, respectively; [12]), thus making coral skeleton a relatively poor heat conductor.

However, this value could vary with porosity and the relative content of water and aragonite, and the dimensions and size of the skeleton could also affect the conduction heat flux [2].

These results appear paradoxical in light of the greater resistance of massive compared with branching species [52–54]. We speculate that during low spring tides, when exposed to low flow conditions and elevated irradiance, massive species may tolerate regular exposures to temperatures greater than previously thought. This greater thermal tolerance perhaps results from the superior acclimatization capacity of slow-growing massive species compared with fast-growing branching species [55]. The history of previous thermal or light exposure can shape the response to thermal stress, either by physiological acclimatization or selective adaptation [5,52,56–59]. For instance, the worldwide range of coral thermal tolerance correlates with ambient water temperatures, thus indicating that corals have adapted to ambient conditions [4,5,60]. Additionally, bleaching impacts are often less in shallow reef environments that regularly experience large diurnal fluctuations in temperature during low-tide periods, compared with deeper and thermally more stable habitats [37,61]. Finally, at the scale of individual colonies, regular exposure to stressful conditions of elevated irradiance can enhance the physiological tolerance to elevated temperature and irradiance [58,62]. It is thus possible that differences in the history of thermal exposure caused by frequent solar heating may influence coral acclimatization. This should be further investigated, as it may affect our understanding of the fundamental differences in the physiology of bleaching sensitive and resistant species.

4.4. Heat versus mass transfer

This first experimental comparison between heat and mass transfer at the surface of symbiont-bearing corals revealed a discrepancy between the heat and mass transfer exponents (figure 7), which challenges expectations from the theoretical analogy between heat and mass transfer. The heat transfer exponent (figure 7) was approximately 0.5 for both coral species, indicative of a laminar boundary layer [22], whereas the exponent for O_2 transfer (figure 7) was close to 0.7, indicative of mass transfer across a turbulent boundary layer [22].

While it is true that measurements of the TBL and the DBL were not performed simultaneously (all corals were sampled for the TBL first and the procedure was then repeated for the DBL), care was taken to preserve the position and orientation of each coral within the flow chamber, as well as the sampled region on the colony. The thickness of boundary layers can vary with the exact location around the colony ([22]; figure 3), particularly in the case of developing boundary layers [63], and thus small variations in the experimental configuration could have affected boundary layer measurements. However, we would expect such variability to occur randomly within both experiments, and to affect TBL and DBL measurements in a similar way.

The presence of a microsensor can induce a local compression of the boundary layer [64], most probably owing to a local acceleration of the flow. However, the relative size of the sensor tip (50 and 10 μm for temperature and O_2, respectively) and the boundary layer (1000 and 200 μm for TBL and DBL, respectively, at 2 cm s^{-1}; figure 7) was similar for both TBL and DBL measurements; thus, we would expect a similar effect on both boundary layers. However, a direct quantification of microsensor-induced boundary layer compression effects on TBLs remains to be done.

Both heat and mass transfer processes are ultimately governed by the momentum boundary layer, which is caused by the interaction between the flow regime and the coral's surface [23]. Results from this study appear as a major discrepancy in light of the analogy between heat and mass transfer, as a single exponent was expected to describe the effect of flow on the thickness of the TBL and DBL. Complementary measurements of the velocity profiles within the momentum boundary layer would be required to fully characterize transport processes at the surface of corals.

Interestingly, the distinct exponents measured in this study for heat and mass transfer, while at odds within a single momentum boundary layer, are each consistent with expectations from heat transfer theory and previous measurements on corals. The heat transfer exponent of approximately 0.5 is consistent with predictions from engineering studies of similar geometric shapes [12]. By contrast, the mass transfer exponent (approx. 0.7) is significantly higher than the value of 0.5 expected from heat transfer theory over the covered range of the Reynolds number (less than 10 000), but is consistent with previous reports of enhanced O_2 transfer across the DBL of corals [6,16,23] where the mass exponent ranged from 0.9 to 2.4.

Surface O_2 flux, and thus O_2 concentration profiles within the DBL, may be affected by chemical and biological processes at the surface of corals, such as carbonate chemistry or enzymatic activity [19], and photorespiration [65]. DBLs may also be disrupted by the topographical roughness of skeletal features such as calices and septa [16,66], but it mostly remains unclear why mass transfer is so enhanced at the surface of corals [16], and why, in this study, it appears more efficient than heat transfer.

The apparent discrepancy between heat and mass transfer exponents may also be a result of the different scales of the TBL and DBL (figure 7), which may be differentially affected by small skeletal roughness elements and/or the movement of polyps [32] and coral tissue cilia [16]. In the current experiment, the surface roughness of *S. pistillata* had no effect on the TBL, whereas Shashar *et al.* [40] demonstrated that small topographical features of *S. pistillata* polyps did affect the structure of the DBL. Simultaneous measurements of O_2 and temperature using a combined O_2–temperature microsensor, together with an assessment of temporal fluctuations in both boundary layers [67], may refine comparisons of heat and mass transfer at the surface of corals.

In conclusion, the present study is the first to compare TBL and DBL characteristics of corals under increasing flow and our results indicate that for topographically complex biological surfaces such as corals, heat and mass transfer should not be treated as completely

analogous processes. Thus, it is difficult and can be misleading to translate between flow effects on the coral TBL and flow effects on the coral DBL, and vice versa. Further studies are needed to understand the mechanisms behind this apparent discrepancy, e.g. by including fine-scale measurements of flow and the momentum boundary layer.

4.5. Extrapolation to field conditions

In this study, coral temperature–flow relationships were characterized under controlled laboratory conditions of steady flow and low velocity ($5\,cm\,s^{-1}$or less). This obviously limits the ability to extrapolate our data to describe the temperature of corals *in situ*, where flows can be spatially and temporally variable, with turbulent eddies and oscillations generated by wave action and the complex three-dimensional structure of the reef (e.g. [42]). Our results are, however, directly applicable to the particular conditions of steadier flows with low velocity and minimal wave action occurring in shallow reef flats or lagoons under calm weather conditions (e.g. [16,44]). As discussed earlier, the temperature of corals is unlikely to exceed that of the surrounding water under stronger flow conditions. However, our experiments realistically reproduced flow conditions relevant to solar-driven warming of shallow-water corals, and the results may help produce realistic estimates of the differences in temperature that may arise between individual corals, in particular during a bleaching event.

Furthermore, the TBL was measured locally on the upper (sun-exposed) surface of the corals and was correlated to the flow velocity measured in the free stream directly above the corals. Therefore, laboratory-based TBL–flow relationships such as these should permit realistic estimates of the local TBL around small colonies and individual branches, provided local flow conditions are measured or modelled (e.g. [68]).

5. CONCLUSION

The TBL over corals such as *Leptastrea* and *Platygyra* sp. can be spatially heterogeneous and affected by the topographical roughness of the skeleton. For topographically smoother corals such as *P. lobata* and *S. pistillata*, coral surface temperature can be described in terms of simple mathematical relationships. A power-law relationship describes the TBL thickness as a function of flow, and this is in turn linearly correlated to the coral's surface temperature. These empirical relationships can be used within a semi-empirical coral thermal model to predict the surface temperature of corals under realistic field conditions of flow and irradiance. The heat exponent characterizing the effect of flow on the TBL is consistent with expectations from engineering studies of simple geometric shapes, but differs from the mass exponent for O_2 transfer across the DBL. Additional TBL and DBL measurements, possibly with a combined oxygen–temperature microsensor, would be required to further investigate the potential for coral behaviour, physiology, or surface topography to differentially affect the TBL and DBL.

We thank N. Ralph for constructing the flow chambers and the staff at Heron Island Research Station for their support. This research was funded by a University of Technology Sydney, institutional grant (P.J.R.) and a grant by the Danish Natural Science Research Council (M.K.) The research was conducted under Great Barrier Reef Marine Park Authority permits G05/16166.1, G07/24174.1 and G03/12019.1.

REFERENCES

1 Fabricius, K. E. 2006 Effects of irradiance, flow, and colony pigmentation on the temperature microenvironment around corals: implications for coral bleaching? *Limnol. Oceanogr.* **51**, 30–37. (doi:10.4319/lo.2006.51.1.0030)
2 Jimenez, I. M., Kühl, M., Larkum, A. W. D. & Ralph, P. J. 2008 Heat budget and thermal microenvironment of shallow-water corals: do massive corals get warmer than branching corals? *Limnol. Oceanogr.* **53**, 1548–1561. (doi:10.4319/lo.2008.53.4.1548)
3 Glynn, P. W. 1993 Coral reef bleaching: ecological perspectives. *Coral Reefs* **12**, 1–17. (doi:10.1007/BF00303779)
4 Coles, S. L., Jokiel, P. L. & Lewis, C. R. 1976 Thermal tolerance in tropical versus subtropical pacific reef corals. *Pac. Sci.* **30**, 159–166.
5 Coles, S. L. & Brown, B. E. 2003 Coral bleaching—capacity for acclimatization and adaptation. *Adv. Mar. Biol.* **46**, 183–223. (doi:10.1016/S0065-2881(03)46004-5)
6 Lesser, M. P., Weis, V. M., Patterson, M. R. & Jokiel, P. L. 1994 Effects of morphology and water motion on carbon delivery and productivity in the reef coral, *Pocillopora damicornis* (Linnaeus): diffusion barriers, inorganic carbon limitation, and biochemical plasticity. *J. Exp. Mar. Biol. Ecol.* **178**, 153–179. (doi:10.1016/0022-0981(94)90034-5)
7 Wilkinson, C. R. 1999 Global and local threats to coral reef functioning and existence: review and predictions. *Mar. Freshw. Res.* **50**, 867–878. (doi:10.1071/MF99121)
8 Wilkinson, C. R. (ed.) 2004 *Status of coral reefs of the world: 2004*. Townsville, Australia: Global Coral Reef Monitoring Network and Australian Institute of Marine Science.
9 Hoegh-Guldberg, O. 1999 Climate change and world's coral reefs: implications for the Great Barrier Reef. *Mar Freshw. Res.* **50**, 839–866. (doi:10.1071/MF99078)
10 Strong, A. E., Arzayus, F., Skirving, W. & Heron, S. F. 2006 Identifying coral bleaching remotely via Coral Reef Watch—improved integration and implications for changing climate. In *Coral reefs and climate change—science and management* (eds J. T. Phinney, O. Hoegh-Guldberg, J. Kleypas, W. Skirving & A. Strong) pp. 163–180. Coastal and Estuarine Studies 61. Washington, DC: American Geophysical Union.
11 Gates, D. M. 1980 *Biophysical ecology*. New York, NY: Courier Dover Publications.
12 Incropera, F. P. & Dewitt, D. P. 1996 *Fundamentals of heat and mass transfer*, 4th edn. New York, NY: Wiley.
13 Kühl, M., Cohen, Y., Dalsgaard, T., Jørgensen, J. B. B. & Revsbech, N. P. 1995 Microenvironment and photosynthesis of zooxanthellae in scleractinian corals studied with microsensors for O_2, pH and light. *Mar. Ecol. Progr. Ser.* **117**, 159–172. (doi:10.3354/meps117159)
14 Shashar, N., Kinane, S., Jokiel, P. L. & Patterson, M. R. 1996 Hydromechanical boundary layers over a coral reef. *J. Exp. Mar. Biol. Ecol.* **199**, 17–28. (doi:10.1016/0022-0981(95)00156-5)
15 Dade, W. B., Hogg, A. J. & Boudreau, B. P. 2001 Physics of flow above the sediment-water interface. In *The benthic*

boundary layer: transport processes and biogeochemistry (eds B. P. Boudreau & B. B. Jørgensen), pp. 4–43. Oxford, UK: Oxford University Press.
16 Patterson, M. R., Sebens, K. P. & Olson, R. R. 1991 *In situ* measurements of flow effects on primary production and dark respiration in reef corals. *Limnol. Oceanogr.* **36**, 936–948. (doi:10.4319/lo.1991.36.5.0936)
17 Kelley, R. 2009 Indo Pacific Coral Finder. See www.byo-guides.com.
18 Nishihara, G. N. & Ackerman, J. D. 2006 The effect of hydrodynamics on the mass transfer of dissolved inorganic carbon to the freshwater macrophyte *Vallisneria americana*. *Limnol. Oceanogr.* **51**, 2734–2745. (doi:10.4319/lo.2006.51.6.2734)
19 Nishihara, G. N. & Ackerman, J. D. 2007 On the determination of mass transfer in a concentration boundary layer. *Limnol. Oceanogr: Methods* **5**, 88–96. (doi:10.4319/lom.2007.5.88)
20 Hochberg, E. J., Atkinson, M. J., Apprill, A. & Andréfouët, S. 2004 Spectral reflectance of coral. *Coral Reefs* **23**, 84–95. (doi:10.1007/s00338-003-0350-1)
21 Enriquez, S., Mendez, E. R. & Iglesias-Prieto, R. 2005 Multiple scattering on coral skeletons enhances light absorption by symbiotic algae. *Limnol. Oceanogr.* **50**, 1025–1032. (doi:10.4319/lo.2005.50.4.1025)
22 Schlichting, H. 1979 *Boundary-layer theory*. New York, NY: McGraw-Hill.
23 Patterson, M. R. & Sebens, K. P. 1989 Forced convection modulates gas exchange in cnidarians. *Proc. Natl. Acad. Sci. USA* **86**, 8833–8836. (doi:10.1073/pnas.86.22.8833)
24 Gardella, D. J. & Edmunds, P. J. 1999 The oxygen microenvironment adjacent to the tissue of the scleractinian *Dichocoenia stokesii* and its effects on symbiont metabolism. *Mar. Biol.* **135**, 289–295. (doi:10.1007/s002270050626)
25 Finelli, C., Helmuth, B., Pentcheff, N. & Wethey, D. 2006 Water flow influences oxygen transport and photosynthetic efficiency in corals. *Coral Reefs* **25**, 47–57. (doi:10.1007/s00338-005-0055-8)
26 Atkinson, M. J. & Bilger, R. W. 1992 Effects of water velocity on phosphate uptake in coral reef-flat communities. *Limnol. Oceanogr.* **37**, 273–279. (doi:10.4319/lo.1992.37.2.0273)
27 Baird, M. E. & Atkinson, M. J. 1997 Measurement and prediction of mass transfer to experimental coral reef communities. *Limnol. Oceanogr.* **42**, 1685–1693. (doi:10.4319/lo.1997.42.8.1685)
28 Thomas, F. I. M. & Atkinson, M. J. 1997 Ammonium uptake by coral reefs: Effects of water velocity and surface roughness on mass transfer. *Limnol. Oceanogr.* **42**, 81–88. (doi:10.4319/lo.1997.42.1.0081)
29 Patterson, M. R. 1991 The effects of flow on polyp-level prey capture in an octocoral, *Alcyonium siderium*. *Biol. Bull.* **180**, 93–102. (doi:10.2307/1542432)
30 Helmuth, B. S. T. & Sebens, K. P. 1993 The influence of colony morphology and orientation to flow on particle capture by the scleractinian coral *Agaricia agaricites* (Linnaeus). *J. Exp. Mar. Biol. Ecol.* **165**, 251–278. (doi:10.1016/0022-0981(93)90109-2)
31 Sebens, K. P., Witting, J. & Helmuth, B. 1997 Effects of water flow and branch spacing on particle capture by the reef coral *Madracis mirabilis* (Duchassaing and Michelotti). *J. Exp. Mar. Biol. Ecol.* **211**, 1–28. (doi:10.1016/S0022-0981(96)02636-6)
32 Dennison, W. C. & Barnes, D. J. 1988 Effect of water motion on coral photosynthesis and calcification. *J. Exp. Mar. Biol. Ecol.* **115**, 67–77. (doi:10.1016/0022-0981(88)90190-6)
33 De Beer, D., Kühl, M., Stambler, N. & Vaki, L. 2000 A microsensor study of light enhanced Ca^{2+} uptake and photo-synthesis in the reef-building coral *Favia* sp. *Mar. Ecol. Progr. Ser.* **194**, 75–85. (doi:10.3354/meps194075)
34 Nakamura, T., Van Woesik, R. & Yamasaki, H. 2005 Photoinhibition of photosynthesis is reduced by water flow in the reef-building coral *Acropora digitifera*. *Mar. Ecol. Prog. Ser.* **301**, 109–118. (doi:10.3354/meps301109)
35 Nakamura, T. & Van Woesik, R. 2001 Water-flow rates and passive diffusion partially explain differential survival of corals during the 1998 bleaching event. *Mar. Ecol. Prog. Ser.* **212**, 301–304. (doi:10.3354/meps212301)
36 Nakamura, T., Yamasaki, H. & Van Woesik, R. 2003 Water flow facilitates recovery from bleaching in the coral *Stylophora pistillata*. *Mar. Ecol. Prog. Ser.* **256**, 287–291. (doi:10.3354/meps256287)
37 West, J. & Salm, R. 2003 Resistance and resilience to coral bleaching: implications for coral reef conservation and management. *Conserv. Biol.* **17**, 956–967. (doi:10.1046/j.1523-1739.2003.02055.x)
38 Brown, B. E. 1997 Coral bleaching: causes and consequences. *Coral Reefs* **16**, 129–138. (doi:10.1007/s003380050249)
39 Jokiel, P. L. 2004 Temperature stress and coral bleaching. In *Coral health and disease* (eds E. Rosenberg & Y. Loya), pp. 401–425. Berlin, Germany: Springer.
40 Shashar, N., Cohen, Y. & Loya, Y. 1993 Extreme diel fluctuations of oxygen in diffusive boundary layers surrounding stony corals. *Biol. Bull.* **185**, 455–461. (doi:10.2307/1542485)
41 Ulstrup, K., Ralph, P. J., Larkum, A. W. D. & Kühl, M. 2006 Intra-colonial variability in light acclimation of zooxanthellae in coral tissues of *Pocillopora damicornis*. *Mar. Biol.* **149**, 1325–1335. (doi:10.1007/s00227-006-0286-4)
42 Monismith, S. G. 2007 Hydrodynamics of coral reefs. *Annu. Rev. Fluid Mech.* **39**, 37–55. (doi:10.1146/annurev.fluid.38.050304.092125)
43 Sebens, K. P. 1997 Adaptive responses to water flow: morphology, energetics, and distribution of reef corals. *Proc. Eighth Int. Coral Reef Symp.* **2**, 1053–1058.
44 Smith, L. W. & Birkeland, C. 2007 Effects of intermittent flow and irradiance level on back reef *Porites* corals at elevated seawater temperatures. *J. Exp. Mar. Biol. Ecol.* **341**, 282–294. (doi:10.1016/j.jembe.2006.10.053)
45 Kraines, S., Yanagi, T., Isobe, M. & Komiyama, H. 1998 Wind-wave driven circulation on the coral reef at Bora Bay, Miyako Island. *Coral Reefs* **17**, 133–143. (doi:10.1007/s003380050107)
46 Ulstrup, K. E., Hill, R. & Ralph, P. J. 2005 Photosynthetic impact of hypoxia on *in hospite* zooxanthellae in the scleractinian coral *Pocillopora damicornis*. *Mar. Ecol. Prog. Ser.* **286**, 125–132. (doi:10.3354/meps286125)
47 Chamberlain, J. A. J. & Graus, R. R. 1975 Water flow and hydromechanical adaptations of branched reef corals. *Bull. Mar. Sci.* **25**, 112–125.
48 Fitt, W. K., Mcfarland, F. K., Warner, M. E. & Chilcoat, G. C. 2000 Seasonal patterns of tissue biomass and densities of symbiotic dinoflagellates in reef corals and relation to coral bleaching. *Limnol. Oceanogr.* **45**, 677–685. (doi:10.4319/lo.2000.45.3.0677)
49 Apprill, A. M., Bidigare, R. R. & Gates, R. D. 2007 Visibly healthy corals exhibit variable pigment concentrations and symbiont phenotypes. *Coral Reefs* **26**, 387–397. (doi:10.1007/s00338-007-0209-y)
50 Ulstrup, K. E., Hill, R., Van Oppen, M. J. H., Larkum, A. W. D. & Ralph, P. J. 2008 Seasonal variation in the photo-physiology of homogeneous and heterogeneous *Symbiodinium* consortia of two scleractinian corals. *Mar.*

Ecol. Prog. Ser. **361**, 139–150. (doi:10.3354/meps07360)
51 Piggot, A. M., Fouke, B. W., Sivaguru, M., Sanford, R. A. & Gaskins, H. R. 2009 Change in zooxanthellae and mucocyte tissue density as an adaptive response to environmental stress by the coral, *Montastraea annularis*. *Mar. Biol.* **156**, 2379–2389. (doi:10.1007/s00227-009-1267-1)
52 Marshall, P. A. & Baird, A. H. 2000 Bleaching of corals on the Great Barrier Reef: differential susceptibilities among taxa. *Coral Reefs* **19**, 155–163. (doi:10.1007/s003380000086)
53 Loya, Y., Sakai, K., Yamazato, K., Nakano, Y., Sambali, H. & Van Woesik, R. 2001 Coral bleaching: the winners and the losers. *Ecol. Lett.* **4**, 122–131. (doi:10.1046/j.1461-0248.2001.00203.x)
54 Stimson, J., Sakai, K. & Sembali, H. 2002 Interspecific comparison of the symbiotic relationship in corals with high and low rates of bleaching-induced mortality. *Coral Reefs* **21**, 409–421. (doi:10.1007/S00338-002-0264-3)
55 Gates, R. D. & Edmunds, P. J. 1999 The physiological mechanisms of acclimatization in tropical reef corals. *Am. Zool.* **39**, 30–43. (doi:10.1093/icb/39.1.30)
56 Jokiel, P. L. & Coles, S. L. 1990 Response of Hawaiian and other Indo-Pacific reef corals to elevated temperature. *Coral Reefs* **8**, 155–162. (doi:10.1007/BF00265006)
57 Craig, P., Birkeland, C. & Belliveau, S. 2001 High temperatures tolerated by a diverse assemblage of shallow-water corals in American Samoa. *Coral Reefs* **20**, 185–189. (doi:10.1007/S003380100159)
58 Brown, B., Dunne, R., Goodson, M. & Douglas, A. 2002 Experience shapes the susceptibility of a reef coral to bleaching. *Coral Reefs* **21**, 119–126. (doi:10.1007/S00338-002-0215-7)
59 Maynard, J., Anthony, K., Marshall, P. & Masiri, I. 2008 Major bleaching events can lead to increased thermal tolerance in corals. *Mar. Biol.* **155**, 173–182. (doi:10.1007/s00227-008-1015-y)
60 Berkelmans, R. 2002 Time-integrated thermal bleaching thresholds of reefs and their variation on the Great Barrier Reef. *Mar. Ecol. Progr. Ser.* **229**, 73–82. (doi:10.3354/meps229073)
61 Hoeksema, B. W. 1991 Control of coral bleaching in mushroom coral populations (Scleractinia: Fungiidae) in the Java Sea): stress tolerances and interference by life history strategy. *Mar. Ecol. Progr. Ser.* **74**, 225–237. (doi:10.3354/meps074225)
62 Brown, B. E., Downs, C. A., Dunne, R. P. & Gibb, S. W. 2002 Exploring the basis of thermotolerance in the reef coral *Goniastrea aspera*. *Mar. Ecol. Progr. Ser.* **242**, 119–129. (doi:10.3354/meps242119)
63 Nishihara, G. N. & Ackerman, J. D. 2009 Diffusive boundary layers do not limit the photosynthesis of the aquatic macrophyte, *Vallisneria americana*, at moderate flows and saturating light levels. *Limnol. Oceanogr.* **54**, 1874–1882. (doi:10.4319/lo.2009.54.6.1874)
64 Glud, R., Gundersen, J., Revsbech, N. & Jørgensen, B. 1994 Effects on the benthic diffusive boundary layer imposed by microelectrodes. *Limnol. Oceanogr.* **39**, 462–467. (doi:10.4319/lo.1994.39.2.0462)
65 Mass, T., Genin, A., Shavit, U., Grinstein, M. & Tchernov, D. 2010 Flow enhances photosynthesis in marine benthic autotrophs by increasing the efflux of oxygen from the organism to the water. *Proc. Natl Acad. Sci. USA* **107**, 2527–2531. (doi:10.1073/pnas.0912348107)
66 Gardella, D. J. & Edmunds, P. J. 2001 The effect of flow and morphology on boundary layers in the scleractinians *Dichocoenia stokesii* (Milne-Edwards and Haime) and *Stephanocoenia michilini* (Milne-Edwards and Haime). *J. Exp. Mar. Biol. Ecol.* **256**, 279–289. (doi:10.1016/S0022-0981(00)00326-9)
67 Jørgensen, B. B. & Des Marais, D. J. 1990 The diffusive boundary layer of sediments: Oxygen microgradients over a microbial mat. *Limnol. Oceanogr.* **35**, 1343–1355. (doi:10.4319/lo.1990.35.6.1343)
68 Kaandorp, J. A., Koopman, E. A., Sloot, P. M. A., Bak, R. P. M., Vermeij, M. J. A. & Lampmann, L. E. H. 2003 Simulation and analysis of flow patterns around the scleractinian coral *Madracis mirabilis* (Duchassaing and Michelotti). *Phil. Trans. R. Soc. Lond. B* **358**, 1551–1557. (doi:10.1098/rstb.2003.1339)